Measurement of the Effective Thickness of the Mucosal Unstirred Layer in *Necturus* Gallbladder Epithelium

CALVIN U. COTTON and LUIS REUSS

From the Department of Physiology and Biophysics, The University of Texas Medical Branch, Galveston, Texas 77550

ABSTRACT The effective thickness of the unstirred fluid layer (USL) adjacent to an epithelial barrier can be estimated from the time course for the accumulation or depletion of a solute at the membrane surface. In 1985 we reported an unstirred layer thickness of ~70 μm for *Necturus* gallbladder epithelium. In our earlier studies the delay caused by noninstantaneous bulk solution mixing was not taken into account and thus the USL thickness was systematically overestimated. In the present studies we describe an analysis of the time course of solute arrival at the membrane surface that takes into account noninstantaneous bulk solution mixing. We also describe a simple technique to monitor the accumulation or depletion of a solute at the membrane surface. The time course for the change in the concentration of either tetramethylammonium (TMA^+) or tetrabutylammonium (TBA^+) upon elevation of bulk solution concentration is sensed at the membrane surface with an ion-sensitive microelectrode. Because of the high selectivity of the ion-sensitive resin for TMA^+ or TBA^+ over other monovalent cations in the solution (Na^+ and K^+), a low concentration (1–2 mM) of the probe can be used. By measuring the time course of the arrival of first one probe and then the other, under identical superfusion conditions, sufficient information is obtained to eliminate multiple fits to the data, obtained when only one probe is used. Neglecting bulk solution mixing caused an error >50% in estimated apparent USL thickness. The effective thickness of the USL depends critically upon chamber geometry, flow rate, and the position of superfusion and suction pipettes. Under our experimental conditions the effective USL at the mucosal surface of *Necturus* gallbladder epithelium was ~40 μm.

INTRODUCTION

The existence of unstirred fluid layers (USLs) in biological systems has been acknowledged by a number of investigators, but their importance in physiologic experiments has not always been appreciated. Many of the problems and artifacts resulting from unstirred layers in biological preparations are described and discussed in detail in the excellent review by Barry and Diamond (1984). For instance,

Address reprint requests to Dr. Calvin U. Cotton, Department of Physiology and Biophysics, The University of Texas Medical Branch, Galveston, TX 77550.

J. GEN. PHYSIOL. © The Rockefeller University Press · 0022-1295/89/04/0631/17 $2.00
Volume 93 April 1989 631–647

transmembrane fluxes of highly permeant species may be significantly reduced by USL, resulting in large errors in estimates of the true membrane permeability. In addition, serious underestimates of membrane osmotic water permeability have been attributed to accumulation or depletion of solute in the USL adjacent to epithelial membranes. Wilson and Dietschy (1974) measured the kinetics of uptake of bile acids, sugars, and an amino acid into intestinal segments at different solution stirring rates (to produce a range of effective USL thicknesses). They found that unstirred layers introduced major errors into the determination of K_m and J_{max} for active transport processes.

Several methods have been described to estimate the effective thickness of unstirred layers. Ginzburg and Katchalsky (1963) measured the apparent diffusional water permeability of cellulose membranes at different stirring speeds. If a value is assumed for the tortuosity of the pathway of water permeation through the cellulose membrane, then the true permeability of the membrane and the thickness of the USL can be estimated. Although reasonable estimates of the tortuosity of hydrated cellulose membranes may be obtained, such approximations are of little value in biological membranes. Andreoli and Troutman (1971) measured the apparent permeability of an artificial lipid membrane to water, urea, and glycerol at different solution viscosities. Since the diffusion coefficient is inversely related to the viscosity of the solution, the USL thickness could be calculated. Green and Otori (1970) measured the USL thickness adjacent to a contact lens and to a cornea mounted in a chamber by direct visualization of the motion of small latex particles. Dainty and House (1966) and Diamond (1966) calculated the USL thickness from the time course for the buildup or depletion of a solute adjacent to an epithelial barrier. However, this approach is valid only when the concentration of the probe in the bulk solution is changed instantaneously (i.e., as a step function). Any gradual change in bulk solution concentration will result in an overestimate of the USL thickness. The magnitude of the error depends upon the rate of bulk solution mixing, the thickness of the USL, and the diffusion coefficient of the probe molecule.

In the present experiments we demonstrate the error introduced by noninstantaneous bulk solution mixing in the estimation of the effective thickness of the USL adjacent to a planar biological membrane. In addition, we describe a simple method that provides a more accurate determination of effective USL thickness. We describe this method for *Necturus* gallbladder epithelium; however, it should be generally applicable to any planar epithelium in which extracellular microelectrodes can be placed near the surface of the tissue. A major advantage of this method when used in conjunction with intracellular microelectrode techniques is that the measurement is at the site of recording in contrast with methods which yield an average value for the surface.

METHODS

Tissue and Solutions

Necturus maculosus were maintained in aquaria at 5–10°C. The animals were anesthetized by immersion in a 1 g/liter solution of tricaine methanesulfate. Gallbladders were removed, opened, rinsed free of bile, and mounted apical side up in the chamber depicted in Fig. 1.

The lower compartment was closed, had a volume of ~0.8 ml, and was perfused at a flow rate of 10–15 ml/min. The upper compartment of the chamber was open, had a volume of ~0.2 ml, and was exchanged at a flow rate of 20–30 ml/min. The solution in the mucosal compartment had the shape of a segment of a sphere. Its volume was maintained approximately con-

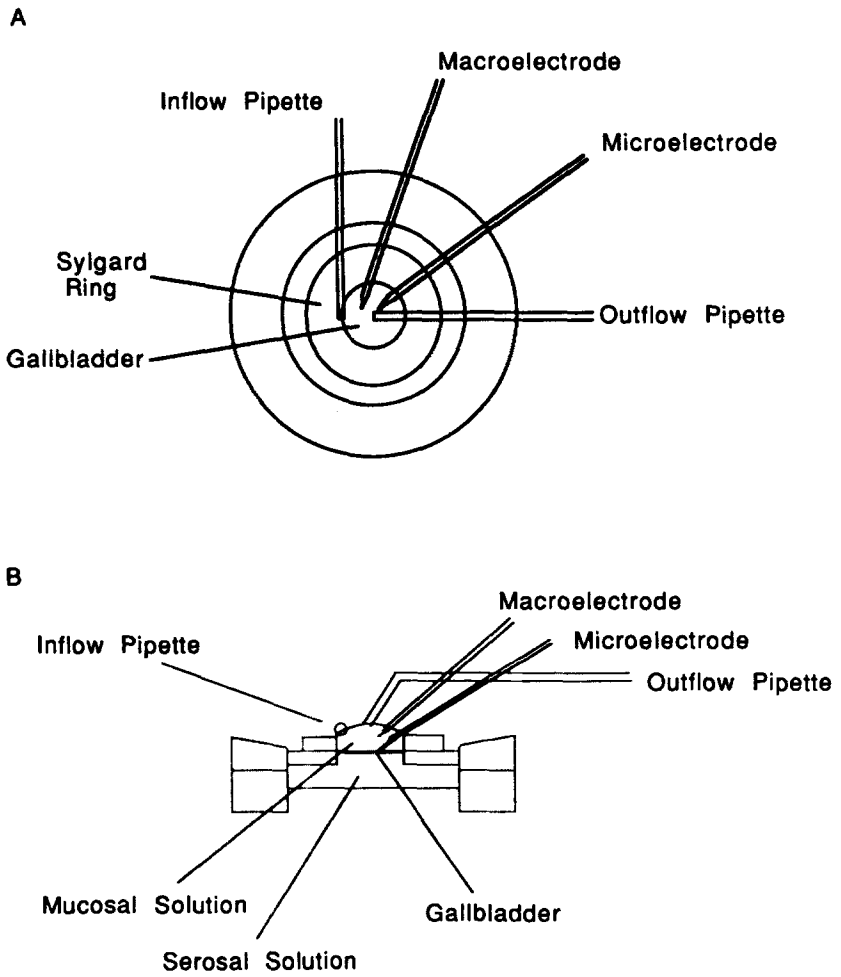

FIGURE 1. Diagram of the perfusion chamber. (*A*) The orientation of the perfusion pipettes and electrodes in the mucosal fluid compartment viewed from above. (*B*) Cross-sectional view of the mucosal and serosal fluid compartments. Note that the inflow pipette is oriented parallel to the tissue and tangential to the dome of mucosal solution. The serosal inflow and outflow pipettes and the reference serosal electrode have been omitted from the diagram. The drawing is not to scale.

stant by rapid superfusion and suction. The inflow pipette was aligned tangentially to the solution's edge, in a plane parallel to the tissue (~1 mm above the tissue). The tip of the suction pipette was positioned at the apex of the segment of sphere. This arrangement was chosen to optimize bulk solution mixing. Mixing was assessed visually with a dye. In some

experiments the inflow pipette was raised to an ~45° angle and directed towards the microelectrode. Solution changes were made by activating a pneumatic valve to exchange two continuous flows of equal rate, one toward the apical compartment of the chamber and the other one to waste. The distance between the valve and the tip of the superfusion pipette was ~6 cm and the solution transit time was 1.0–1.5 s.

The control bathing solution (NaCl Ringer's solution) contained 90 mM NaCl, 10 mM $NaHCO_3$, 2.5 mM KCl, 1.8 mM $CaCl_2$, 1.0 mM $MgCl_2$, and 0.5 mM NaH_2PO_4 and was equilibrated with 1% CO_2/99% air. The pH was ~7.65 and the osmolality was ~200 mosmol/kg. Solutions contained either 1.0 or 2.0 mM tetramethylammonium chloride (TMACl) or tetrabutylammonium chloride (TBACl).

Microelectrode Fabrication and Calibration

Large-tipped, ion-sensitive microelectrodes were prepared from borosilicate glass with internal fiber (1 mm o.d., 0.5 mm i.d., Glass Company of America, Bargaintown, NJ). The micropipettes were pulled (PD 5 microelectrode puller; Narishige, Tokyo, Japan) and the tips were broken under microscopic observation to ~2–4 μm by advancing the pipette with a micromanipulator until the tip touched a polished stainless steel surface. The broken-tip pipettes were placed tip-up on a perforated aluminum block, covered with a glass jar, and baked in an oven at 200° C for at least 2 h. The pipettes were rendered hydrophobic by exposure, in the oven, to hexamethyldisilazane vapor (Sigma Chemical Co., St. Louis, MO) and baked for an additional 1–2 h. The electrode tip was filled with a cocktail that contained potassium tetrakis (*p*-chlorophenylborate) 5 mg in 0.1 ml of 3-nitro-*O*-xylene, and 10% wt/vol polyvinyl chloride. Tetrahydrofuran (~20% vol/vol) was added to reduce the viscosity of the resin (Marban et al., 1980). This ion-sensitive resin is known to have a high selectivity for quarternary ammonium compounds (Neher and Lux, 1973; Reuss, 1985). After filling, the electrodes were allowed to cure for 36–48 h. Incorporation of polyvinyl chloride into the microelectrode cocktail was necessary to polymerize the resin and prevent its loss from the large tip of the microelectrode. The electrodes were backfilled with NaCl Ringer's solution and a chloridized silver wire was inserted and sealed in place with dental wax. Resistances ranged from 1 to 5 GΩ when immersed in NaCl Ringer's solution.

Electrodes were calibrated with solutions that contained NaCl Ringer's solution plus 0.5–10.0 mM TMACl or TBACl. Electrode slopes ranged from 56 to 62 mV/log [TMA^+] or [TBA^+]. The selectivity ratios measured with pure salt solutions (0.5, 1.0, and 2.0 mM) were $TMA^+/K^+ = 10^2$ to 10^3, $TMA^+/Na^+ = 10^3$ to 10^4, TBA^+/Na^+ and $TBA^+/K^+ > 10^6$.

Electrical Measurements

The transepithelial voltage (V_{ms}) was measured as the difference between an Ag-AgCl pellet connected to the lower compartment of the chamber with a Ringer/agar bridge (reference) and a calomel half-cell in series with a flowing, saturated KCl macroelectrode constructed from a fiber-filled glass pipette (Ultrawick; World Precision Instruments, New Haven, CT) pulled to a tip diameter ~1 mm which was placed in the upper compartment, next to the suction (outflow) pipette. At the superfusion rates used, the KCl leak into the mucosal solution compartment did not elicit measurable elevations in K^+ activity. The ion-sensitive microelectrode was connected to a high input-impedance electrometer (model FD-223; World Precision Instruments). The Ag-AgCl pellet in the lower compartment served as ground. The extracellular cation-sensitive microelectrode was positioned within 1–3 μm of the apical cell membrane with a hydraulic micromanipulator (model MO-103, Narishige). The tissue was observed with a microscope (Diavert, E. Leitz, Inc., Rockleigh, NJ) equipped with Hoffman modulation-contrast optics at a magnification of 300. Transepithelial voltage (V_{ms}) and differ-

ential ion-sensitive electrode voltage ($V_{TMA^+} - V_{ms}$ or $V_{TBA^+} - V_{ms}$) were amplified, displayed on an oscilloscope, digitized (instrument computer model 1074; Nicolet Instrument Corp., Madison, WI) and stored (Northstar Horizon Microcomputer, San Leandro, CA) for subsequent analysis. Each channel was sampled at 100 Hz.

Calculations and Data Analysis

The differential ion-sensitive voltage ($V_i - V_{ms}$) at each time point (100 Hz) was converted to a concentration according to Eq. 1:

$$C(t) = C(0)\ 10^{(\Delta V/s)}, \tag{1}$$

where $C(t)$ = concentration of TMA^+ or TBA^+ at a time = t (mM), $C(0)$ = concentration of TMA^+ or TBA^+ at time = 0 (=1 mM), $\Delta V = [(V_i - V_{ms})(t) - (V_i - V_{ms})(0)]$ (mV), and s = electrode slope (mV/log concentration).

The fractional concentration of TMA^+ or TBA^+ was calculated for each time point according to Eq. 2:

$$FC(t) = \frac{C(t) - C(0)}{C(\infty) - C(0)}, \tag{2}$$

where $C(t)$ = concentration of TMA^+ or TBA^+ at time = t (mM), $C(0)$ = concentration of TMA^+ or TBA^+ at time = 0 (=1 mM), and $C(\infty)$ = concentration of TMA^+ or TBA^+ at steady state after solution change (=2 mM).

The data, expressed as fractional concentrations, were transferred to a VAX computer (Digital Equipment Corp., Maynard, MA) for curve fitting to the appropriate model equations (see below).

The data were fit to two equations initially devised to describe heat transfer in solid bodies, but which are also appropriate for diffusion problems. In the first model we assume an unstirred solution layer in which solute fluxes are diffusive. The layer is modeled as a slab of height δ, bounded on one side by a planar membrane (the apical surface of the epithelium) that is impermeable to the probe (TMA^+ or TBA^+) and on the other by a perfectly mixed bulk solution compartment. Furthermore, fluxes of water across the membrane are neglected. We also assume infinite volume for the bulk solution. Finally, we assume that at both $t = 0$ and $t = \infty$ the probe has the same concentration throughout the apical solution compartment, i.e., in bulk solution and unstirred layer. At $t = 0$ the concentration of the probe in the bulk solution is instantaneously raised (step function) from 1.0 to 2.0 mM. Certainly, this condition is not met in our experiments, but we present this approach because it has been widely used. A more appropriate model without this constraint is presented below (see Eqs. 5A and 5B). For the case of a step change in bulk solute concentrations, the time course for the concentration of the probe in the USL is given by Eq. 3A (see Eq. 8.41, Simon, 1986; equivalent to Eq. 4.17, Crank, 1975).

$$\frac{C_{(x,t+\Delta t)}}{C_{(x,\infty)}} = 1 - \frac{4}{\Pi}\sum_{n=1}^{n=\infty}\frac{(-1)^{(n-1)/2}}{n}\cdot e^{-(n\Pi/2\delta)^2 D(t+\Delta t)}\cdot\cos\left(\frac{n\Pi x}{2\delta}\right), \tag{3A}$$

where $C(x, t + \Delta t)$ = concentration of TMA^+ or TBA^+ at distance x from the membrane at time = t (mM), $C(x, \infty)$ = concentration of TMA^+ or TBA^+ in bulk solution after the instantaneous increase (mM), $N = 1, 3, 5 \ldots$, δ = unstirred layer thickness (cm), $\Pi = 3.1416$, D = diffusion coefficient for TMACl (1.39×10^{-5} cm^2/s) or TBACl (0.76×10^{-5} cm^2/s), t = time (s), Δt = an increment in time that allows us to experimentally identify $t = 0$ (s), x = distance between measurement site and membrane surface (in centimeters).

Although the microelectrode is not precisely at the membrane surface, we attempted to place the tip near the surface by first advancing it until contact with the epithelial surface was made and then withdrawing by 1–3 μm. Contact was determined electrically, i.e., by noting a DC offset in the oscilloscope trace upon contact of the microelectrode tip with the tissue surface, and optically (Leitz inverted microscope equipped with Hoffman modulation-contrast optics, magnification 300). Since we could not accurately determine the distance from the membrane, we assume $x = 0$; therefore, Eq. 3A simplifies to 3B:

$$\frac{C_{(t+\Delta t)}}{C_{(\infty)}} = 1 - \frac{4}{\Pi}\sum_{n=1}^{n=\infty}\frac{(-1)^{(n-1)/2}}{n}\cdot e^{-(n\Pi/2\delta)^2 D(t+\Delta t)}. \tag{3B}$$

By defining $t_{1/2}$ as the time at which $C_{(t)} = (C_{(\infty)} - C_{(0)})/2$, the following relationship holds,

$$\delta^2 = \frac{t_{1/2}\,D}{0.38}. \tag{4}$$

This equation is used to calculate USL thickness in some experiments. The second model to which our data are fit is identical to the first model described above except the bulk solution concentration of the probe does not increase instantaneously, but instead increases exponentially at the bulk solution/USL interface with a time constant τ. In other words, we assume homogenous mixing of the bulk solution (except for the unstirred layer). This situation is described by Eq. 5A. (see Eq. 10, Austin, 1932):

$$\frac{C_{(x,t+\Delta t)}}{C_{(x,\infty)}} = 1 - e^{-(t+\Delta t)/\tau} - \frac{e^{-(t+\Delta t)/\tau}}{\tau}\sum_{m=1}^{m=\infty} A\,\frac{\cos\left(\frac{Qx}{\delta}\right)}{D\left(\frac{Q}{\delta}\right)^2 - \frac{1}{\tau}}\cdot\left\{1 - e^{-[D(Q/\delta)^2 - 1/\tau](t+\Delta t)}\right\}, \tag{5A}$$

where τ = time constant for the change in probe concentration at the interface between the bulk solution and the USL (s), $m = 1, 2, 3, \ldots$, $A = 4(-1)^{1+m}/\Pi(2m-1)$, $Q = (2m-1)\Pi/2$.

Again, if the measurement is made at the surface of the epithelium, i.e., at $x = 0$, Eq. 5A reduces to Eq. 5B:

$$\frac{C_{(t+\Delta t)}}{C_{(\infty)}} = 1 - e^{-(t+\Delta t)/\tau} - \frac{e^{-(t+\Delta t)/\tau}}{\tau}\sum_{m=1}^{m=\infty} A\,\frac{1}{D\left(\frac{Q}{\delta}\right)^2 - \frac{1}{\tau}}\cdot\left\{1 - e^{-[D(Q/\delta)^2 - 1/\tau](t+\Delta t)}\right\}. \tag{5B}$$

As in the preceding model, we assume that there are no probe concentration differences between bulk solution and unstirred layer at either $t = 0$ or $t = \infty$. The data are the calculated fractional concentrations [$FC(t)$, see Eq. 2] sampled at a rate of 100 Hz. These data were fit to appropriate forms of Eq. 3B and/or 5B and the resultant values for δ, Δt, and τ were determined. The fitting routine was a grid-search least-squares fit for nonlinear functions (Bevington, 1969). Since the series converges rapidly for values of $FC(t) > 0.01$, 30 terms (i.e., $n = 1$–59 for Eq. 3B and $m = 1$–30 for Eq. 5B) were sufficient for even very small values of $FC(t)$.

The value of χ^2 was calculated from Eq. 6:

$$\chi^2 = \frac{1}{N}\sum_{i=1}^{N}[f(x)_i^{obs} - f(x)_i^{exp}]^2, \tag{6}$$

where N = number of data points, $f(x)_i^{obs}$ = observed value of fractional accumulation at $(x)_i$, $f(x)_i^{exp}$ = expected value of fractional accumulation at $(x)_i$.

Since the data span the same range (i.e., 0.0–1.0), the values of χ^2 obtained from fitting a given data set to Eq. 3B or Eq. 5B may be compared directly. Since the data variance is the

same, a lower value of χ^2 indicates a better fit. In the model described by Eq. 3B there are two free parameters (Δt and δ), whereas in the model corresponding to Eq. 5B there are three free parameters. (Δt, δ, and τ). Addition of a third parameter will by itself result in an equally good or improved fit. We will provide evidence that inclusion of the time constant for mixing in the bulk solution is justified both on experimental and statistical grounds. For each fit we computed an R factor, which expresses the percent misfit between the theoretical curve and the data, according to Eq. 7:

$$R^2 = \frac{\sum_{i=1}^{N} [f(x)_i^{obs} - f(x)_i^{exp}]^2}{\sum_{i=1}^{N} [f(x)_i^{obs}]^2} \tag{7}$$

A test statistic (F_x) was calculated from Eq. 8:

$$F_x = (R_1^2 - R_0^2)/R_0^2, \tag{8}$$

where the subscripts 1 and 0 refer to the fits with two and three parameters, respectively.

The significance of the value of F_x was assessed from the F-distribution with degrees of freedom $\nu_1 = 1$ and $\nu_2 = N - 3$, where ν_1 is the difference in the number of parameters between the two fits and ν_2 is the number of data points minus the large number of parameters. If $F_x > F$, we conclude that statistically the additional parameter merits inclusion in the model (Bevington, 1969).

RESULTS

The time course for the accumulation of TMA^+ near the apical membrane of the gallbladder epithelium is illustrated in Fig. 2. The TMA^+ concentration in the bulk

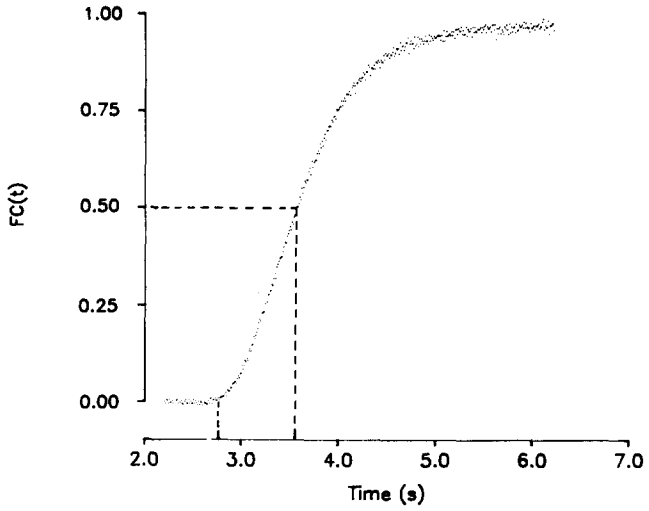

FIGURE 2. Time course for the change in [TMA^+] at the cell membrane. At $t = \sim 2$ s the mucosal perfusate was changed from NaCl Ringer plus 1 mM TMACl to NaCl Ringer plus 2 mM TMACl. TMA^+ was sensed by an extracellular microelectrode placed near the apical cell membrane and voltages were sampled at 100 Hz. The fractional concentration [$FC(t)$] of TMA^+ was calculated from Eqs. 1 and 2. The effective unstirred layer thickness (δ) in this experiment was calculated from Eq. 4. The $t_{1/2}$ was 0.8 s and yielded a $\delta = 54$ μm.

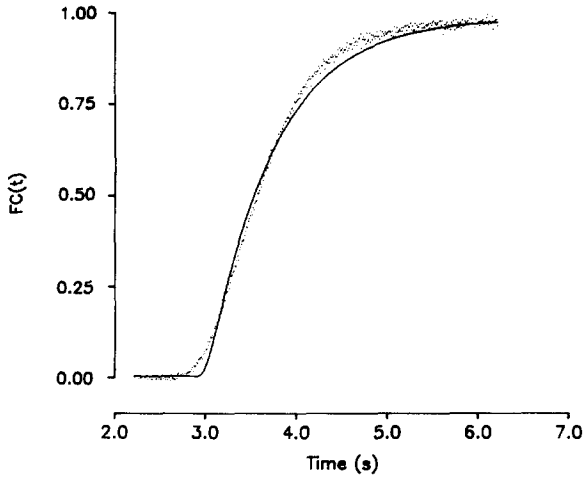

FIGURE 3. Time course for the change in [TMA^+] at the cell membrane (*dots*) and best fit (*solid line*) to the data using the model described by Eq. 3B, i.e., assuming a step change in bulk [TMA^+]. The values for the fitted parameters are $\delta = 50$ μm and $\Delta t = -2.84$ s ($\chi^2 = 5.77 \times 10^{-4}$). Inasmuch as the data are the same as shown in Fig. 2, the estimates of δ may be directly compared.

solution was increased from 1 to 2 mM and the effective thickness of the unstirred layer, calculated from Eq. 4, i.e., from the time required to achieve a TMA^+ concentration of 1.5 mM at the cell surface, is 55 μm.

The same trace was further evaluated at the cell surface by fitting the data to the model which assumes a step change in bulk solution concentration and for which the concentration at $x = 0$ is described by Eq. 3B. The data and the fitted curve are shown in Fig. 3. This analysis yielded an estimate of effective USL thickness of 50 μm. If this value of δ is used to calculate the time course for the arrival to the apical surface of another ion (TBA^+) with a different diffusion coefficient, the agreement

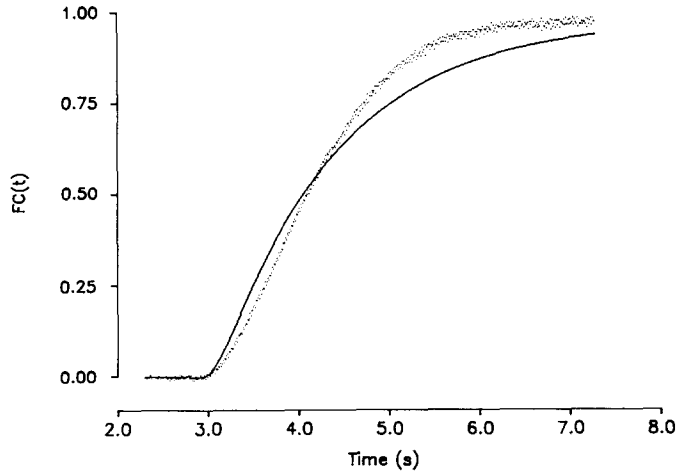

FIGURE 4. Observed (*dots*) and predicted (*solid line*) time courses for the change in [TBA^+] at the cell membrane. The superfusion conditions were identical to those described in Fig. 2, except that TBA^+ was the probe. The predicted time course was generated by fitting the data with the step-change model described by Eq. 3B. The value of δ (50 μm) was taken from the best fit in Fig. 3 and was fixed; $\Delta t = -2.80$ s and $\chi^2 = 3.31 \times 10^{-3}$.

between the predicted and the observed time courses is not good (see Fig. 4). The TMA^+ trace (Fig. 3) and the TBA^+ trace (Fig. 4) were obtained sequentially under identical fluid exchange conditions. Furthermore, fitting the TBA^+ data to Eq. 3B yields a best fit with an effective USL of 42 μm, which on inspection is clearly not a good fit (Fig. 5).

The poor fits illustrated in Figs. 3 and 5, and the inability to accurately predict the time course for the arrival of a solute with a different diffusion coefficient (Fig. 4) result from violation of a crucial requirement of the model, namely that the bulk solution concentration be changed instantaneously. This condition is not met experimentally. The magnitude of the error depends on the relative contributions of delays due to bulk mixing and diffusion in the USL to the time course of the concentration changes in the USL. For a fixed mixing pattern and USL thickness, the error is larger for more rapidly diffusing substances. It is therefore necessary to

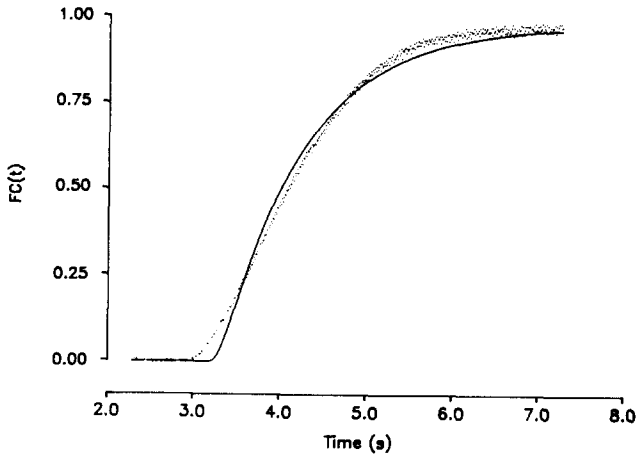

FIGURE 5. Time course for the change in $[TBA^+]$ at the cell membrane (*dots*) and best fit (*solid line*) to the data using the step-change model described by Eq. 3B. The values for the fitted parameters are $\delta = 42$ μm and $\Delta t = -3.11$ s ($\chi^2 = 7.48 \times 10^{-4}$).

include explicitly in the model an expression for the time constant for the change in probe concentration at the interface between the bulk solution and the USL (i.e., time constant for the mixing in the bulk solution compartment).

This was done by assuming that such mixing can be described by a single exponential of time constant τ. Accordingly, the data depicted in Fig. 3 were fit to the model described by Eq. 5B, which includes τ. The result, illustrated in Fig. 6 *A*, was a much better fit than that obtained in Fig. 3. The effective USL thickness is 37 μm and the time course of bulk solution mixing (τ) is 0.46 s. This value for τ agrees well with that calculated (τ') from the superfusion rate and the mucosal solution volume (τ' = volume/flow rate = 0.2 ml/[0.33 ml/s] = 0.6 s), assuming ideal mixing in the bulk solution. Additional evidence for the appropriateness of this model is provided by the analysis of the TBA^+ data shown in Fig. 4. The results are illustrated in Fig. 6 *B*, which clearly depicts a better fit than that obtained in Fig. 4. The effective USL

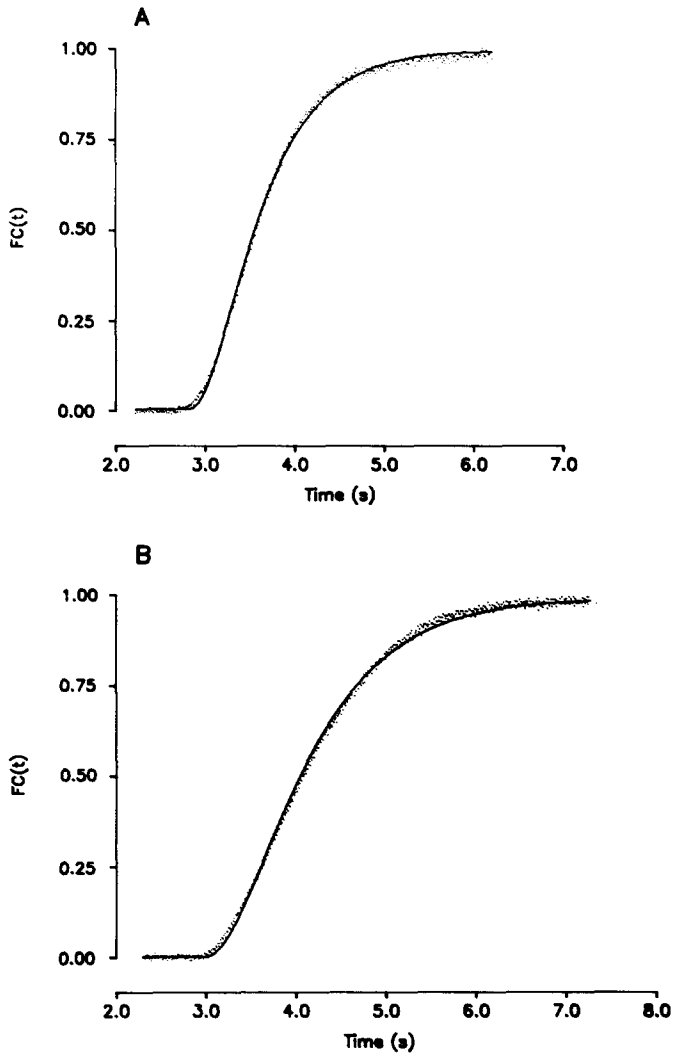

FIGURE 6. (*A*) Time course for the change in $[TMA^+]$ at the cell membrane (*dots*) and best fit (*solid line*) to the data assuming an exponential change in bulk solution concentration (model described by Eq. 5B). The values for the fitted parameters are $\delta = 37$ μm, $\tau = 0.46$ s, and $\Delta t = -2.74$ s ($\chi^2 = 1.21 \times 10^{-4}$). (*B*) Time course for the change in $[TBA^+]$ (*dots*) and best fit (*solid line*) using Eq. 5B. The values for the fitted parameters are $\Delta = 34$ μm, $\tau = 0.62$ s, and $\Delta t = 2.89$ s ($\chi^2 = 1.43 \times 10^{-4}$). The values of δ and τ in *A* and *B* can be compared since the traces were obtained sequentially under identical superfusion conditions.

thickness is 34 μm and the time constant for bulk solution mixing is 0.62 s. These values agree well with those obtained from the TMA^+ trace (Fig. 6 *A*). In a series of four consecutive solution changes in which pipette and microelectrode position and solution flow rates were kept constant, the estimates of δ and τ varied by <10%.

However, if the position of the inflow pipette and/or the flow rate are altered, the estimate of δ can be quite different (see below).

It is possible to reduce the USL thickness in the region of measurement to near zero by aiming the inflow pipette at the tip of the microelectrode. This is illustrated in Fig. 7 for both TMA^+ (*A*) and TBA^+ (*B*). The estimates of USL thickness (Eq. 5B) are 8 and 15 μm for the TMA^+ and TBA^+ traces, respectively, the time constants for

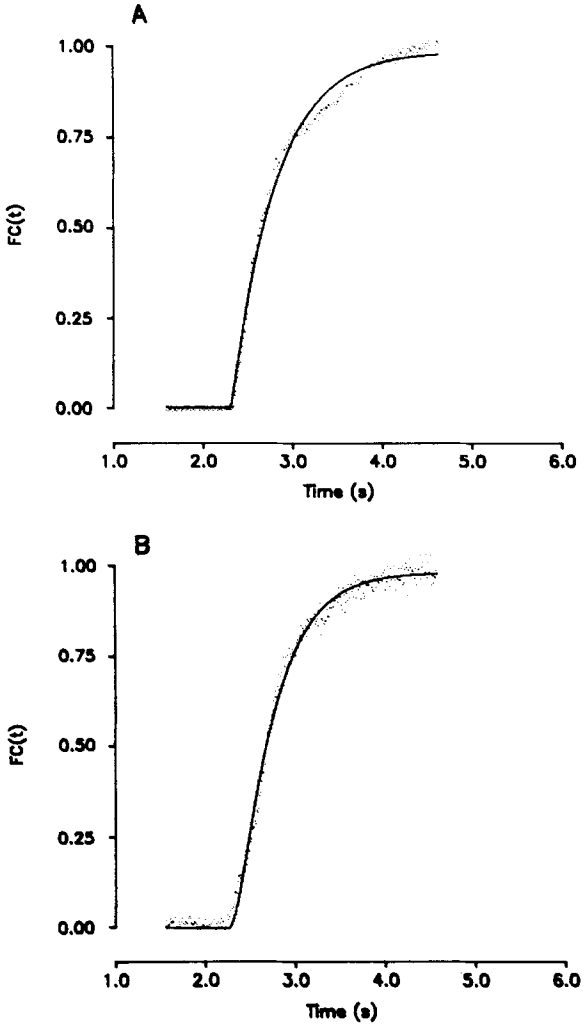

FIGURE 7. Time course for the change in (*A*) [TMA^+] or (*B*) [TBA^+] at the cell membrane with the solution inflow aimed at the electrode tip. (*A*) Experimental data (*dots*) and best fit (*solid line*) using Eq. 5B (exponential change in bulk solution concentrations). The values for the fitted parameters are $\delta = 8$ μm, $\tau = 0.48$ s, and $\Delta t = -2.31$ s ($\chi^2 = 7.35 \times 10^{-4}$). (*B*) Experimental data (*dots*) and best fit (*solid line*) using Eq. 5B. The values for the fitted parameters are $\delta = 15$ μm, $\tau = 0.39$ s, and $\Delta t = -2.27$ s ($\chi^2 = 7.09 \times 10^{-4}$). The values of δ and τ in *A* and *B* can be compared since the traces were obtained sequentially under identical superfusion conditions.

bulk solution mixing are 0.48 and 0.39 s for TMA^+ and TBA^+ traces, respectively. Although changing the position of the superfusion pipette clearly alters the time course for the change in solute concentration at the membrane surface, note that in experiments in which only the position of the inflow pipette was changed the values for τ were similar (see Figs. 6, *A* and *B*, and 7, *A* and *B*). The increase in apparent

noise in the data from experiments in which the inflow pipette was aimed at the microelectrode suggest that there may be turbulence at or near the electrode tip, since a similar "noisy" response is observed when the electrode tip is elevated to a large distance (>100 μm) above the surface of the tissue, or when it is placed directly in the path of fluid flow.

DISCUSSION

Recognition of the existence of unstirred fluid layers in biological preparations and of the experimental problems that arise as a consequence of these fluid layers has led investigators to pursue one of two approaches. First, the effective USL thickness can be estimated and appropriate corrections can be applied to the data. Alternatively, the exchange rate or stirring rate of the solution may be increased to minimize the USL thickness. The latter approach has resulted in minimal unstirred layer thickness in isolated, perfused renal tubules (see, e.g., Strange and Spring, 1986), but it is not always applicable since solution turbulence and/or high-velocity perfusion may cause unacceptable displacement in the tissue, such as movement sufficient to preclude use of intracellular microelectrode recording techniques. Furthermore, anatomic constraints, such as those imposed by intestinal crypts or subepithelial connective tissue, may prevent effective mixing near the membrane of interest. These considerations justify the need for design and use of accurate and precise methods to estimate USL thickness in flat epithelia and in other planar membrane preparations.

Many of the methods that have been described to measure USL thickness are not easy to apply to biological preparations. For instance, the approach described by Andreoli and Troutman (1971) required a broad range of solution viscosities and a membrane with a high permeability for the test solute. The most frequently used technique in epithelial preparations is the method described independently by Dainty and House (1966) and by Diamond (1966). These authors measured the transepithelial streaming potentials or biionic diffusion potentials that result from unilateral addition of sucrose or replacement of Na^+ by K^+, respectively. Since the voltage transients arise as a consequence of changes in solute concentration at the membrane, the time course of the voltage change can be used to calculate USL thickness. The measurement can be made with the tissue mounted in a traditional "Ussing-type" flux chamber. This is important since the USL thickness will vary with mixing conditions and chamber geometry. In a recent theoretical article, Pedley (1983) has discussed the adequacy of the approach outlined by Dainty and House (1966) and Diamond (1966). Pedley correctly points out that this model for USLs assumes a linear concentration profile, and consequently a distinct interface between well-mixed (bulk) and unmixed (USL) fluids. Pedley advocates an analytic solution specific for each pattern of mixing of the bulk solution. As will be discussed below, the approach described by Dainty and House (1966) and by Diamond (1966) can, with appropriate modifications, yield an accurate and experimentally useful estimate of effective USL thickness.

We previously used a modification of the method of Dainty and House (1966) and Diamond (1966) to estimate the USL thickness of *Necturus* gallbladder epithe-

lium (Cotton and Reuss, 1985; Reuss, 1985). In those studies the USL thickness was estimated from either the change in apical membrane voltage or the response of a K^+-selective microelectrode, placed near the apical cell membrane, to an elevation of apical solution K^+ concentration. The time required to elevate $[K^+]$ at the membrane surface by 50% of the final change ($t_{1/2}$) was determined, and δ was calculated from Eq. 4, i.e., the special case for the $t = t_{1/2}$ of diffusion into or out of a slab of solution upon a step change in concentration at the surface (Eq. 3B).

The approach presented in this paper takes advantage of the time and space resolution provided by ion-sensitive microelectrodes to measure the chemical activity of appropriate probes. In principle, the presence of the microelectrode by itself could affect the bulk solution mixing or diffusion of the probe through the USL. To prevent such artifacts, the microelectrodes were positioned at a relatively flat angle (~30° with respect to the tissue) thus, the shaft of the microelectrode was not in the convective-diffusive path from the inflow pipette to the cell surface. We reported an effective USL thickness of ~70 μm (range 25–100 μm). Eqs. 3B and 4 are appropriate only if several assumptions, outlined in Methods, are met. First, the membrane must be impermeable to the probe. Inasmuch as the *Necturus* gallbladder epithelium is essentially impermeable to TMA^+ and TBA^+, this condition is met. Secondly, the volume of the bulk solution must be infinite and well mixed. Since the tissue is superfused, the volume of solution is effectively infinite and the pattern of dye mixing in the chamber suggests rapid and complete mixing. Finally, the concentration of the probe in the bulk solution must be changed instantaneously (i.e., as a step function). This assumption is clearly not met in the experiment and results in a systematic overestimate of the value of δ. The most likely source of the error is that the time course of probe accumulation is determined by both bulk solution mixing and diffusion through the unstirred fluid layer.

A modified form of Eq. 3A is presented in Carslaw and Jaeger (1959, p. 104, Eq. 5). This equation can be applied to the time course of accumulation of a solute at a membrane when the change in bulk solution concentration is not instantaneous. However, this equation was derived for the case of an exponential change in solute concentration in the bulk solution that is rapid relative to the time required for diffusion through the USL. This requirement is not met in our experimental preparation since the half-times for bulk solution mixing (~0.35 s for a $\tau = 0.5$ s) and for diffusion across an USL of ~40 μm (0.44 s for TMA^+ and 0.80 s for TBA^+) are of similar magnitude.

Our data were fit to a modified form of a more general solution formulated by Austin (Austin, 1931; Austin, 1932, Eq. 10) to describe heat conduction in a solid when the surface temperature is increased or decreased exponentially. Since in our experiments it was not easy to accurately determine $t = 0$ (Eq. 5B), we added a parameter "Δt," which allowed the fitted curve to "slide" along the time axis without a change in shape. Several observations suggest that inclusion of a parameter (τ) to describe mixing in the bulk solution is necessary. First, poor fits were obtained when the data were fitted to the model that assumed an instantaneous change in concentration in the bulk solution (Eq. 3B; Figs. 3 and 5). Secondly, with the step-change model it was not possible to accurately predict the time course of the concentration of a solute with a different diffusion coefficient (Fig. 4). Thirdly, a theo-

retical calculation of the time constant of the chamber (based upon flow rate and volume) suggested that bulk solution mixing could not be ignored. Fourthly, if an ion-sensitive microelectrode is placed at a height of ~70 μm above the epithelium (i.e., beyond the USL) and the concentration of the probe is increased, the resulting time course is not a step change, but instead a single exponential with a time constant (τ) of ~0.35 s (data not shown). For a volume of 0.2 ml and a flow rate of 0.5 ml·s^{-1}, the estimated time constant was 0.4 s. Finally, our approach is validated by the agreement of the fitted curve with the data and by the similarity of the values for USL thickness (δ) and for the time constant of bulk solution mixing (τ) determined from fits to data sets obtained with either TMA^+ or TBA^+ as probes (Fig. 6, *A* and *B*).

During the course of these experiments we discovered that there was not always a unique fit to the data. This is not surprising since changes in two of the parameters, τ and δ, produce qualitatively similar effects on the time course for solute buildup at the membrane surface. For example, increases in the values of δ or τ tend to flatten the curve, whereas decreases in the values of either parameter cause the curve to become steeper. A series of solutions was generated by varying τ and δ. For this simulation Δt was fixed at zero and the diffusion coefficient for TMA^+ was used. Although curves *1* (δ = 50 μm, τ = 1.0 s) and *2* (δ = 55 μm, τ = 0.85 s) in Fig. 8 are not identical, they would yield equally acceptable fits to a data set. However, if the values of δ and τ for the two curves that overlap in Fig. 8 (curves *1* and *2*) are used to generate curves for a probe with a different diffusion coefficient (e.g., TBA^+ instead of TMA^+), a clear separation between the curves is obtained (curves *3* and *4*). This exercise indicates that it is possible to obtain unique solutions for τ and δ by using two different probe molecules sequentially while maintaining the same pattern and rate of superfusion, and also the position of the microelectrode.

In principle, if τ could be determined experimentally multiple mathematical solu-

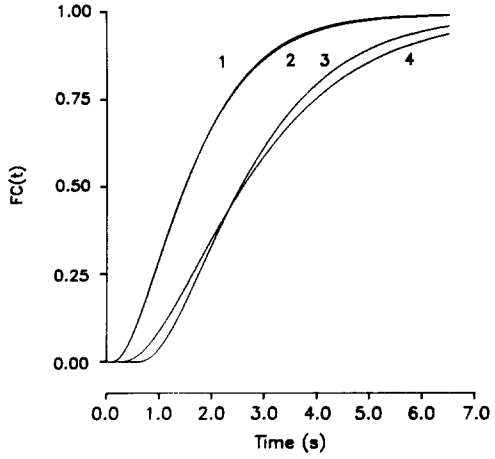

FIGURE 8. Elimination of multiple solutions by the use of two different probes. Curve *1* was generated by solving Eq. 5B for D_{TMA} = 1.39 × 10^{-5} cm^2/s, δ = 50 μm, τ = 1.0 s, and Δt = 0 s. Curve *2* was generated for D_{TMA} = 1.39 × 10^{-5} cm^2/s, δ = 55 μm, and τ = 0.85 s, allowing Δt to vary. Overlap of the two curves is visually apparent and χ^2 for the fit of curve *2* to curve *1* is 1.09 × 10^{-5}, indicative of a good fit. The values of the parameters (δ and τ) obtained from curves *1* and *2*, were used to generate curves *3* and *4*, respectively, using TBA^+ as the probe, instead of TMA^+. D_{TBA} = 0.76 × 10^{-5} cm^2/s was used for both curves 3 and 4. Separation of the two curves is apparent and χ^2 for the fit of curve *4* to curve *3* is 1.03 × 10^{-3}, indicative of a poor fit.

tions could be avoided. However, in practice, τ refers to the time constant for the exponential change in probe concentration at the bulk solution/USL interface (see subsection "Calculations and Data Analysis"); thus, such a procedure would be valid only if two conditions are met, namely ideal (homogeneous) mixing of the bulk solutions and constancy of the apparent unstirred layer thickness independent of microelectrode position. Both conditions are difficult to meet experimentally. Clearly, the shape of the unstirred layer depends on the pattern of fluid flow (Pedley, 1983).

It is possible to reduce USL thickness at the site of measurement to a value considerably less than that obtained in Fig. 6, *A* and *B*. This was achieved (Fig. 7) by aiming the inflow pipette at the electrode tip. Although we have used Eq. 5B to obtain estimates of δ and τ for this experiment, the model is not strictly appropriate, since our results suggest that there is turbulent flow at or near the microelectrode tip. Therefore, when the pipette is aimed at the microelectrode tip, this approach provides an upper estimate of USL thickness, and a reasonable estimate for τ.

The magnitude of the error in the estimation of δ if mixing in the bulk solution is assumed to be a step function can be determined by comparison of values of δ calculated from Eqs. 4 and 5B (Fig. 6, *A* and *B*). In this experiment δ was 54 μm (Eq. 4) or 37 μm (Eq. 5B) for TMA^+ or 54 μm (Eq. 4) and 34 μm (Eq. 5B) for TBA^+; thus, the error is ~50%. Similar calculations for the data in Fig. 7, *A* and *B* yield errors of ~300% and ~100% for TMA^+ and TBA^+, respectively. The absolute and fractional errors will vary depending upon the bulk solution mixing properties, the USL thickness, and the diffusion coefficient of the probe selected for the measurement.

It is difficult to make meaningful comparisons between the results of our experiments and those previously reported by other investigators, primarily because of differences in chamber design and perfusion. However, Diamond (1966), Smulders and Wright (1971), Bindslev et al. (1974), and Westergaard and Dietschy (1974) have reported mucosal USL thickness in rabbit gallbladder (calculated from Eq. 4) to be 113, 95, 70, and 110 μm, respectively. We previously reported a value of ~70 μm for the USL thickness of *Necturus* gallbladder calculated from Eq. 4 (Cotton and Reuss, 1985). Under similar experimental conditions we now report an USL thickness of 40 μm ($n = 5$) when the contribution of bulk solution mixing is taken into account (Eq. 5B). Since the values of τ and δ are certainly not experimental constants, we cannot predict the error in the estimate of δ in other preparations. However, it is appropriate to emphasize that failure to consider the contribution of bulk solution mixing will result in systematic overestimates of δ.

In summary, we have described a rapid and simple method for the estimation of effective USL thickness in a planar epithelial preparation. Since our method requires only short exposure of the tissue to low concentrations of TMA^+ and TBA^+, it is unlikely that the transport properties of the preparation will be altered. Furthermore, this method separates explicitly τ and δ and provides an estimate of effective USL thickness at the site of measurement, rather than an average value for the tissue. This advantage is important since it is likely that the USL thickness will vary depending on position on a planar epithelium. For instance, near the chamber wall the USL is probably thicker than in the center of the preparation. As pointed out by Pedley (1983), it is extremely difficult to achieve spatial homogeneity and consequently no single USL thickness can exist in a preparation. Our approach is

particularly useful when used in conjunction with intracellular microelectrode recordings in which the measurement can be made near the recording site. In the following article, we have extended these techniques and used a detectable probe (TBA^+) with a diffusion coefficient similar to that of an osmotic solute (sucrose), thus permitting a continuous estimate of changes in osmolality at the cell surface (Cotton et al., 1989, next article in this issue).

We thank J. Chilton, R. Ratzlaff, and W. C. Law for their assistance with the curve fitting. We also thank P. De Weer, J. Stoddard, Y. Segal and G. Altenberg for discussion and comments, and A. Pearce and O. Hooks for secretarial help.

This research was supported by National Institutes of Health grant DK-38588.

Original version received 16 May 1988 and accepted version received 8 September 1988.

REFERENCES

Andreoli, T. E., and S. L. Troutman. 1971. An analysis of unstirred layers in series with "tight" and "porous" lipid bilayer membranes. *Journal of General Physiology.* 57:464–478.

Austin, J. B. 1931. Temperature distribution in solid bodies during heating or cooling. *Physics.* 1:75–83.

Austin, J. B. 1932. Temperature distribution in solid bodies during heating or cooling. A correction. *Physics.* 3:179–184.

Barry, P. H., and J. M. Diamond. 1984. Effects of unstirred layers on membrane phenomena. *Physiological Reviews.* 64:763–873.

Bevington, P. R. 1969. Data Reduction and Error Analysis for the Physical Sciences. McGraw-Hill Book Co., Inc., New York. 336 pp.

Bindslev, N., J. McD. Tormey, and E. M. Wright. 1974. The effects of electrical and osmotic gradients on lateral intercellular spaces and membrane conductance in a low resistance epithelium. *Journal of Membrane Biology.* 19:357–380.

Carslaw, H. S., and J. C. Jaeger. 1959. Conduction of Heat in Solids. Clarendon Press, Oxford. 510 pp.

Cotton, C. U., and L. Reuss. 1985. Measurement of the effective thickness of the mucosal unstirred layer in *Necturus* gallbladder epithelium. *Journal of General Physiology.* 86:44a. (Abstr.)

Crank, J. 1975. The Mathematics of Diffusion. Oxford University Press, Oxford. 414 pp.

Dainty, J., and C. R. House. 1966. 'Unstirred layers' in frog skin. *Journal of Physiology.* 182:66–78.

Diamond, J. M. 1966. A rapid method for determining voltage-concentration relations across membranes. *Journal of Physiology.* 183:83–100.

Green, K., and T. Otori. 1970. Direct measurement of membrane unstirred layers. *Journal of Physiology.* 207:93–102.

Ginzburg, B. Z., and A. Katchalsky. 1963. The frictional coefficients of the flows of non-electrolytes through artificial membranes. *Journal of General Physiology.* 47:403–418.

House, C. R. 1974. Water Transport in Cells and Tissues. Edward Arnold Ltd., London. 562 pp.

Marban, E., T. J. Rink, R. W. Tsien, and R. Y. Tsien. 1980. Free calcium in heart muscle at rest and during contraction measured with Ca^{2+}-sensitive microelectrodes. *Nature.* 286:845–850.

Neher, E., and H. D. Lux. 1973. Rapid changes of potassium concentration at the outer surface of exposed single neurons during membrane current flow. *Journal of General Physiology.* 61:385–399.

Pedley, T. J. 1983. Calculation of unstirred layer thickness in membrane transport experiments: a survey. *Quarterly Review of Biophysics.* 16:115–150.

Reuss, L. 1985. Changes in cell volume measured with an electrophysiologic technique. *Proceedings of the National Academy of Sciences.* 82:6014–6018.

Simon, W. 1986. Mathematical Techniques for Biology and Medicine. Dover Publications, New York. 295 pp.

Smulders, A. P., and E. M. Wright. 1971. The magnitude of nonelectrolyte selectivity in the gallbladder epithelium. *Journal of Membrane Biology.* 5:297–318.

Strange, K., and K. R. Spring. 1986. Methods for imaging renal tubule cells. *Kidney International.* 30:192–200.

Westergaard, H., and J. M. Dietschy. 1974. Delineation of the dimensions and permeability characteristics of the two major diffusion barriers to passive mucosal uptake in the rabbit intestine. *Journal of Clinical Investigation.* 54:718–732.

Wilson, F. A., and J. M. Dietschy. 1974. The intestinal unstirred layer: its surface area and effect on active transport kinetics. *Biochimica et Biophysica Acta.* 363:112–126.